On the interest of a space-time regularization for reconstructing sparse excitation sources

Mathieu Aucejo, Olivier de Smet, Jean-François Deü

On the interest of a space-time regularization for reconstructing sparse excitation sources

Mathieu Aucejo, Olivier De Smet and Jean-François Deü

Laboratoire de Mécanique des Structures et des Systèmes Couplés, Conservatoire National des Arts et Métiers, 2 rue Conté, 75003 Paris

E-mail: mathieu.aucejo@lecnam.net

Abstract. In time domain, force reconstruction problems are commonly solved from Tikhonov and LASSO regularizations. Practically, these approaches can lead to inaccurate reconstructions, if the sources to identify don't share the same space-time characteristics or the corresponding force vector doesn't exhibit the desired structure. To alleviate this potential drawback, we have recently introduced a multiplicative space-time regularization that allows exploiting one's prior knowledge of the spatial distribution of the sources as well as their time history. In this contribution, the proposed regularization strategy is compared to the multiplicative Tikhonov and LASSO regularizations through an experimental application to point out the practical interest of exploiting simultaneously both spatial and temporal prior information in terms of quality and robustness of the reconstructed excitation sources.

1. Introduction

Force reconstruction problems in time domain still remain an active topic in the structural dynamics community. To solve this problem, several approaches have been developed, such as Kalman filtering [1] or adaptive filtering [2]. However, the most widespread strategy is certainly the regularization, and more particularly, the Tikhonov and LASSO regularizations. From a theoretical standpoint, Tikhonov regularization should be used when the force signal exhibits a certain continuity [3, 4] and the spatial distribution of the sources is rather smooth [5]. On the contrary, LASSO regularization should be used when the excitation signal is rather impulsive [6, 7] and the spatial distribution of the sources is sparse [8]. It results that classical strategies developed in the literature are theoretically not always well adapted to tackle both the localization and time reconstruction problems at the same time, except for configurations where the force vector to identify has the desired structure or the spatial distribution of sources and the nature of the excitation signals share the same space-time characteristics, such as the sparsity [9]. To the best of our knowledge, only a few methods have been developed to address this specific issue and they generally consist in solving the space-time reconstruction problem in a separated manner [10].

In this contribution, we propose to highlight the practical interest of exploiting simultaneously both the spatial and temporal features of excitation sources to solve the inverse problem efficiently thanks to the multiplicative space-time regularization, recently introduced by the authors [11]. To this end, the proposed regularization strategy is compared to the multiplicative Tikhonov and LASSO regularizations through an experimental application. In particular, it is

shown that properly exploiting one's prior knowledge of the sources to identify allows improving the quality and the robustness of the regularized solutions.

2. Multiplicative space-time regularization

Regularization consists in including in the formulation of the inverse problem some prior information on the excitation field to identify in order to constrain the space of solutions. In the present contribution, it is proposed to seek the unknown global excitation field $\mathbf{F}$ as the solution of the following minimization problem:

$$\widehat{\mathbf{F}} = \underset{\mathbf{F}\setminus\{\mathbf{0}\}}{\operatorname{argmin}}\, \mathcal{F}(\mathbf{Y}-\mathbf{H}\mathbf{F}) \cdot \mathcal{R}(\mathbf{F}), \tag{1}$$

where

- $\mathcal{F}(\mathbf{Y}-\mathbf{H}\mathbf{F})$ is the data-fidelity term which controls the a priori on the noise corrupting the data. Here, it is assumed that the reconstruction model is linear and defined such that:

$$\mathbf{Y} = \mathbf{H}\mathbf{F}; \tag{2}$$

- $\mathcal{R}(\mathbf{F})$ is the regularization term that encodes prior information on the excitation field $\mathbf{F}$, i.e. what is known about the excitation field before making any measurement.

It should be noted here that the previous minimization problem is referred to as multiplicative regularization. This choice has been made, because this approach is generally computationally more efficient than its additive counterpart (a.k.a. Tikhonov-like regularization) given that it is free from the preliminary definition of any optimal regularization parameter [14]. That being said, it is clear from Eq. (1) that the quality of the reconstructed excitation field is not only conditioned to the adequacy of the data-fidelity and regularization terms with the actual noise and the actual space-time source characteristics, but also to the quality of the reconstruction model describing the dynamic behavior of the considered structure. That is why, all the ingredients of the method are described separately for the sake of clarity.

2.1. Derivation of the reconstruction model

The reconstruction model given by Eq. (2) can be classically established either from the discretization of the Duhamel's integral or from the discretization of the state-space representation of the mechanical system. In the present paper, the reconstruction model is built from a discretized state-space representation, because it can easily deal with kinematic data of various types (displacement, velocity, acceleration, strain).

The state-space representation is composed of a state equation and an output equation. In this contribution, we propose a state-space model based on the generalized-α integration scheme [15], because this method is unconditionally stable and second-order accurate and minimizes the numerical damping at low frequencies for a given high-frequency damping level.

To derive the state equation from the generalized-α method, let us consider a regular partition of the time domain such that $t_0 < \cdots < t_k < \cdots < t_f$ (t_0 and t_f: initial and final instants) and let $h = t_{k+1} - t_k$ denote the time step size. For a mechanical system described by its mass, stiffness and damping matrices ($\mathbf{M}$, $\mathbf{K}$, $\mathbf{C}$), one has to start from the following equations [16]:

$$\mathbf{M}\,\ddot{\mathbf{d}}_{k+1-\alpha_m} + \mathbf{C}\,\dot{\mathbf{d}}_{k+1-\alpha_f} + \mathbf{K}\,\mathbf{d}_{k+1-\alpha_f} = \mathbf{S_f}\,\mathbf{f}_{k+1-\alpha_f}, \tag{3a}$$

$$\dot{\mathbf{d}}_{k+1} = \dot{\mathbf{d}}_k + (1-\gamma)\,h\,\ddot{\mathbf{d}}_k + \gamma\,h\,\ddot{\mathbf{d}}_{k+1}, \tag{3b}$$

$$\mathbf{d}_{k+1} = \mathbf{d}_k + h\,\dot{\mathbf{d}}_k + \left(\frac{1}{2}-\beta\right) h^2\,\ddot{\mathbf{d}}_k + \beta\,h^2\,\ddot{\mathbf{d}}_{k+1}, \tag{3c}$$

where γ and β are the parameters of the Newmark method, α_m and α_f are two averaging parameters associated to the inertia and internal/external forces, while $\mathbf{d}_k = \mathbf{d}(t_k)$ and $\mathbf{f}_k = \mathbf{f}(t_k)$ are, respectively, the displacement and excitation vectors at time t_k, $\mathbf{S_f}$ being the selection matrix of the excitation degrees of freedom. In the previous equation, the quantity $\mathbf{d}_{k+1-\alpha}$ must be read as:

$$\mathbf{d}_{k+1-\alpha} = (1-\alpha)\,\mathbf{d}_{k+1} + \alpha\,\mathbf{d}_k. \tag{4}$$

For linear systems, it is a common practice to use a modally reduced order model to limit the computational costs. In this regard, when the displacement vector is expanded on its modal basis, the previous equation of motion becomes:

$$\ddot{\mathbf{q}}_{k+1-\alpha_m} + \mathbf{Z_n}\,\dot{\mathbf{q}}_{k+1-\alpha_f} + \mathbf{\Omega}_\mathbf{n}^2\,\mathbf{q}_{k+1-\alpha_f} = \mathbf{\Phi}_\mathbf{n}^T\,\mathbf{S_f}\,\mathbf{f}_{k+1-\alpha_f}, \tag{5a}$$

$$\dot{\mathbf{q}}_{k+1} = \dot{\mathbf{q}}_k + (1-\gamma)\,h\,\ddot{\mathbf{q}}_k + \gamma\,h\,\ddot{\mathbf{q}}_{k+1}, \tag{5b}$$

$$\mathbf{q}_{k+1} = \mathbf{q}_k + h\,\dot{\mathbf{q}}_k + \left(\frac{1}{2}-\beta\right)h^2\,\ddot{\mathbf{q}}_k + \beta\,h^2\,\ddot{\mathbf{q}}_{k+1}, \tag{5c}$$

where $\mathbf{q}_k$ is the generalized displacement, $\mathbf{\Phi_n}$ is the matrix of the mass-normalized mode shapes, $\mathbf{\Omega_n} = \mathrm{diag}(\omega_1, \ldots, \omega_n)$ and $\mathbf{Z_n} = \mathrm{diag}(2\xi_1\omega_1, \ldots, 2\xi_n\omega_n)$, where ω_n and ξ_n are respectively the modal angular frequency and the modal damping ratio of the mode n.

After some manipulations, detailed in Ref. [11], and considering that the state vector $\mathbf{x}_k$ is defined such that $\mathbf{x}_k = [\mathbf{q}_k^T\ \dot{\mathbf{q}}_k^T\ \ddot{\mathbf{q}}_k^T]^T$, we obtain the following state equation:

$$\mathbf{x}_{k+1} = \mathbf{A}\,\mathbf{x}_k + \mathbf{B}^+\,\mathbf{f}_{k+1} + \mathbf{B}^-\,\mathbf{f}_k, \tag{6}$$

where $\mathbf{A}$ is the system matrix, while $\mathbf{B}^-$ and $\mathbf{B}^+$ are the input matrices applied to the force vector at time k and $k+1$.

Regarding the output equation, it can be expressed as:

$$\begin{aligned}\mathbf{y}_k &= \mathbf{S_d}\,\mathbf{d}_k + \mathbf{S_v}\,\dot{\mathbf{d}}_k + \mathbf{S_a}\,\ddot{\mathbf{d}}_k \\ &= \mathbf{S_d}\,\mathbf{\Phi_n}\,\mathbf{q}_k + \mathbf{S_v}\,\mathbf{\Phi_n}\,\dot{\mathbf{q}}_k + \mathbf{S_a}\,\mathbf{\Phi_n}\,\ddot{\mathbf{q}}_k \\ &= \mathbf{O}\,\mathbf{x}_k,\end{aligned} \tag{7}$$

where $\mathbf{y}_k$ is the output vector, $\mathbf{S_d}$, $\mathbf{S_v}$ and $\mathbf{S_a}$ are, respectively, the selection matrices of the displacement, velocity and acceleration data measured on the structure and $\mathbf{O} = [\mathbf{S_d},\ \mathbf{S_v},\ \mathbf{S_a}]\mathbf{\Phi_n}$ is the output matrix.

All things considered, the state-space representation of the dynamical system deriving from the generalized-α method is given by:

$$\begin{cases}\mathbf{x}_{k+1} = \mathbf{A}\,\mathbf{x}_k + \mathbf{B}^+\,\mathbf{f}_{k+1} + \mathbf{B}^-\,\mathbf{f}_k \\ \mathbf{y}_k = \mathbf{O}\,\mathbf{x}_k\end{cases}. \tag{8}$$

At this stage, a last step is required to derive the reconstruction model as defined in Eq. (2). For this purpose, it is first necessary to express the state vector at time t_k from the state and input vectors at times $t_j \leq t_k$. In doing so, it can be shown that the state vector $\mathbf{x}_k$ writes:

$$\mathbf{x}_k = \mathbf{A}^k\,\mathbf{x}_0 + \mathbf{A}^{k-1}\,\mathbf{B}^-\,\mathbf{f}_0 + \sum_{j=1}^{k-1}\mathbf{A}^{k-j-1}\,\mathbf{B}\,\mathbf{f}_j + \mathbf{B}^+\,\mathbf{f}_k, \quad \text{for } t_k > t_0, \tag{9}$$

where $\mathbf{B} = \mathbf{A}\,\mathbf{B}^{+} + \mathbf{B}^{-}$ and $\mathbf{x}_0$ et $\mathbf{f}_0$ are the known initial state and input vectors.

From the previous relation, it results that the output vector $\mathbf{y}_k$, for $t_0 < t_k \leq t_n$ (n: number of time samples), is given by the relation:

$$\mathbf{y}_k = \mathbf{O}\mathbf{A}^k\,\mathbf{x}_0 + \mathbf{O}\mathbf{A}^{k-1}\,\mathbf{B}^{-}\,\mathbf{f}_0 + \sum_{j=1}^{k-1} \mathbf{O}\mathbf{A}^{k-j-1}\,\mathbf{B}\,\mathbf{f}_j + \mathbf{O}\mathbf{B}^{+}\,\mathbf{f}_k. \tag{10}$$

In the end, the proposed reconstruction model simply writes:

$$\mathbf{Y} = \mathbf{H}\,\mathbf{F}, \tag{11}$$

where

$$\mathbf{Y} = \begin{bmatrix} \mathbf{y}_1 \\ \mathbf{y}_2 \\ \mathbf{y}_3 \\ \vdots \\ \mathbf{y}_n \end{bmatrix} - \begin{bmatrix} \mathbf{O}\mathbf{A} \\ \mathbf{O}\mathbf{A}^2 \\ \mathbf{O}\mathbf{A}^3 \\ \vdots \\ \mathbf{O}\mathbf{A}^n \end{bmatrix} \mathbf{x}_0 - \begin{bmatrix} \mathbf{O}\mathbf{B}^{-} \\ \mathbf{O}\mathbf{A}\mathbf{B}^{-} \\ \mathbf{O}\mathbf{A}^2\mathbf{B}^{-} \\ \vdots \\ \mathbf{O}\mathbf{A}^{n-1}\mathbf{B}^{-} \end{bmatrix} \mathbf{f}_0,\ \mathbf{H} = \begin{bmatrix} \mathbf{O}\mathbf{B}^{+} & \mathbf{0} & \cdots & \mathbf{0} \\ \mathbf{O}\mathbf{B} & \mathbf{O}\mathbf{B}^{+} & \ddots & \vdots \\ \vdots & \vdots & \ddots & \mathbf{0} \\ \mathbf{O}\mathbf{A}^{n-2}\mathbf{B} & \mathbf{O}\mathbf{A}^{n-3}\mathbf{B} & \cdots & \mathbf{O}\mathbf{B}^{+} \end{bmatrix},$$

$$\mathbf{F} = \begin{bmatrix} \mathbf{f}_1 \\ \mathbf{f}_2 \\ \mathbf{f}_3 \\ \vdots \\ \mathbf{f}_n \end{bmatrix}.$$

Here, it is important to note that the initial state and input vectors are chosen so that $\mathbf{x}_0 = \mathbf{0}$ and $\mathbf{f}_0 = \mathbf{0}$. In other words, this means that it is compulsory to start the recordings of the output data before exciting the structure.

2.2. General formulation of the reconstruction problem

To obtain consistent reconstructions, it has be seen that a proper choice of the data-fidelity and regularization terms is crucial, since the more the prior information on the noise and the sources is meaningful, the more the confidence in the reconstruction is high [12]. Consequently, developing a particular regularization strategy is equivalent to propose particular data-fidelity and regularization terms. In the present case, this means that the data-fidelity has to reflect one's prior knowledge on the noise corrupting the data, while the regularization term must reflect one's prior knowledge on the spatial and temporal characteristics of the forces to reconstruct.

Regarding the data-fidelity term, a common assumption consists in considering that the measured data are corrupted by an additive Gaussian white noise, leading to a data-fidelity term of the form:

$$\mathcal{F}(\mathbf{Y} - \mathbf{H}\mathbf{F}) = \|\mathbf{Y} - \mathbf{H}\mathbf{F}\|_2^2\,. \tag{13}$$

The choice of the regularization term requires more reflection, since it must encode available information about the space-time characteristics of the excitation field to identify. To this end, it is relevant to define a regularization term based on a mixed $\ell_{p,q}-$norm. Practically, the regularization term is defined such that:

$$\mathcal{R}(\mathbf{F}) = \|\mathbf{F}\|_{p,q}^{q}\,. \tag{14}$$

To better understand the influence of the space-time regularization term in the formulation of the inverse problem, one can represent the unknown force vector $\mathbf{F}$ as a matrix, where the rows correspond to the time signal at a particular location and the columns to the excitation field at a specific instant. In doing so, it comes:

$$\mathbf{F} = [\mathbf{f}_1 \dots \mathbf{f}_j \dots \mathbf{f}_n] = \begin{bmatrix} f_{11} & \cdots & f_{1j} & \cdots & f_{1n} \\ \vdots & & \vdots & & \vdots \\ f_{i1} & \cdots & f_{ij} & \cdots & f_{in} \\ \vdots & & \vdots & & \vdots \\ f_{m1} & \cdots & f_{mj} & \cdots & f_{mn} \end{bmatrix}, \tag{15}$$

where m is the number of reconstruction points of the excitation field.

On the other hand, if one reminds that the mixed $\ell_{p,q}$-norm is defined by:

$$\|\mathbf{F}\|_{p,q} = \left[\sum_{i=1}^{m} \left(\sum_{j=1}^{n} |f_{ij}|^p \right)^{\frac{q}{p}} \right]^{\frac{1}{q}}, \quad \forall\, (p,q) \in \mathbb{R}_+^*, \tag{16}$$

it becomes clear that the proposed regularization term introduces an explicit coupling between the coefficients of $\mathbf{F}$ and allows promoting some structures observed in real signals [13]. To illustrate this particular property of the mixed norms, let us consider the case for which $(p,q) = (2,1)$. In this situation, the matrix $\mathbf{F}$ is supposed to be sparse along the columns (space) and full along the rows (time). In other words, one promotes the spatial sparsity of the excitation field and the continuity of the time signals.

From the foregoing, the general formulation of the proposed space-frequency multiplicative regularization is given by:

$$\widehat{\mathbf{F}} = \underset{\mathbf{F} \setminus \{\mathbf{0}\}}{\operatorname{argmin}} \ \|\mathbf{Y} - \mathbf{H}\mathbf{F}\|_2^2 \cdot \|\mathbf{F}\|_{p,q}^q \,. \tag{17}$$

From a numerical standpoint, the previous formulation is solved from an adapted Iteratively Reweighted Least Squares algorithm described in Ref. [11]. Interesting readers can refer to the latter reference for more details.

3. Hammer impact reconstruction

In this section, the experimental reconstruction of a hammer impact is studied. This application intends to investigate the practical interest of applying the proposed approach for solving force reconstruction problems. The main objective of this real-world application is to demonstrate the advantages of the proposed strategy in terms of identification quality and robustness in operating conditions, compared to regularization strategies based on standard regularization terms.

3.1. Description of the structure under test

The structure under test is a thin aluminum plate of 60 cm in length, 40 cm in width and 6 mm in thickness, clamped along its length in a wooden support. The effective width of the plate resulting from the mounting conditions is 39.1 cm. To perform all the subsequent measurements the system is suspended to a rigid structure through a set of elastic bungee cords [see Fig. 1].

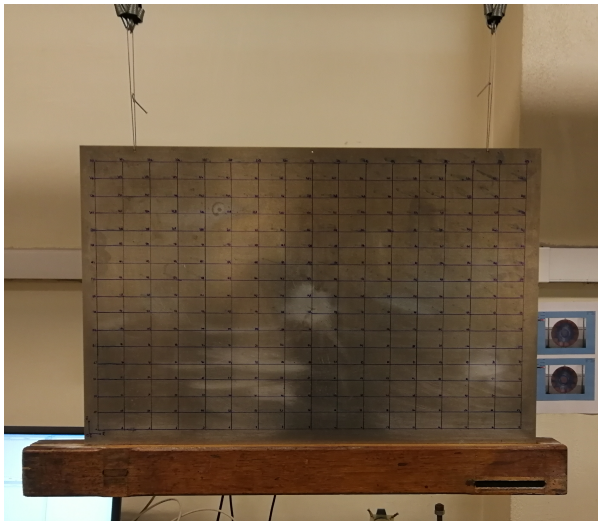

Figure 1: Structure under test

3.2. Reconstruction model
In the present application, the reconstruction model is built from a modal reduction and by considering that only acceleration data are available. Practically, this means that only the modal parameters of the structure and the selection matrix of the acceleration data $\mathbf{S}_\mathrm{a}$ have to be known to establish the reconstruction model given by Eq. (11).

To obtain the modal parameters of the structure, an experimental modal analysis (EMA) has been conducted from a roving hammer test performed on a grid of 17× 17 points using three reference accelerometers and an impact hammer equipped with a steel tip to properly excite all the modes below 6500 Hz. The goal of the EMA is to extract the modes of the real structure in order to limit the influence of modeling errors when establishing the reconstruction model. The locations and the associated identification numbers of the references accelerometers with respect to the measurement grid are presented in Fig. 2. All in all, the first 83 flexible modes and 2 suspension modes (at 1 Hz and 2.5 Hz) have been extracted.

3.2.1. Measurement of acceleration data and excitation signal The output data resulting from a hammer impact have been collected using four accelerometers mounted on the structure. The input and output measurement devices have been located at nodes of the grid defined for the EMA to ensure the consistency of the reconstruction process. The locations and the identification numbers (ID) of the measured input and output data are defined in Fig. 3. In particular, it can be seen that no accelerometer is located at the excitation point (ID: 236).

In the present experiment, the hammer is equipped with a soft rubber tip, so as to fix the cut-off frequency of the excitation around 500 Hz. In this way, the convergence of the reconstruction model in terms of modal series is ensured. Regarding the signal processing parameters, the sampling frequency has been set to 16384 Hz for 32768 lines, meaning that the data have been recorded every 61 μs during 2 s.

3.2.2. Application To demonstrate the interest of including the prior information available about the space-time characteristics of excitation signals, we propose to compare the proposed multiplicative space-time (ST) regularization to the multiplicative counterpart of Tikhonov and

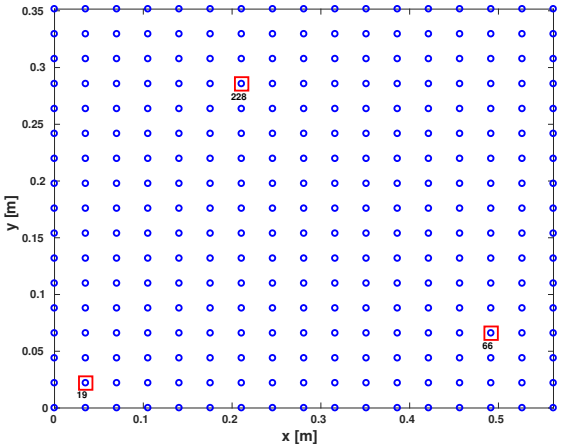

Figure 2: Locations of the reference accelerometers with respect to the grid used for EMA - (○) Roving hammer excitation points and (□) Measurement points (reference accelerometers)

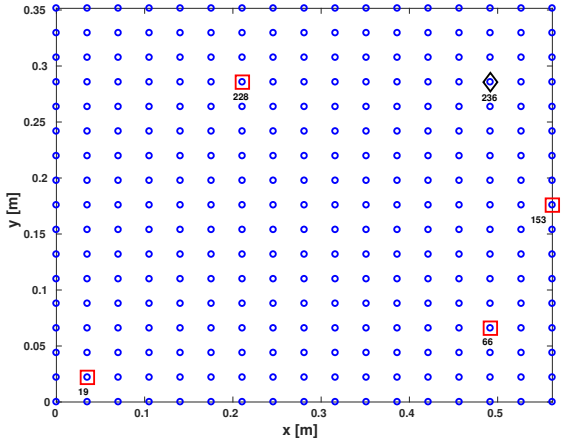

Figure 3: Location of the accelerometers and the hammer impact with respect to grid used for EMA – (○) Nodes of the grid used for EMA, (□) Accelerometers et (◊) Hammer impact

LASSO regularizations. The latter are respectively referred to as multiplicative Tikhonov regularization (mTIK) and multiplicative LASSO (mLASSO) regularization and are formally expressed as:

$$\widehat{\mathbf{F}} = \underset{\mathbf{F}\setminus\{\mathbf{0}\}}{\operatorname{argmin}} \|\mathbf{Y} - \mathbf{H}\mathbf{F}\|_2^2 \cdot \|\mathbf{F}\|_q^q, \tag{18}$$

where $q = 2$ for mTIK and $q = 1$ for mLASSO.

In the following, the reconstructions are performed considering that the acceleration data are measured at nodes 19, 66, 153, 228 of the grid used for the EMA and the excitation sources are identified at nodes 19, 66, 228, 236 [see Fig. 3].

A first comparison is performed by reconstructing the applied forces on a sequence of 24 ms. To apply ST regularization, it is necessary to fix the value of the norm parameters p and q. Because the reconstruction of the hammer impact is performed on a rather short duration, it is

reasonable to promote the continuity of the reconstructed excitation signals and the sparsity of the source distribution on the structure. As a result, the norm parameters defining the space-time regularization term are set to $(p, q) = (2, 0.5)$.

When applying mTIK ($q = 2$), mLASSO ($q = 1$) and ST regularizations on the selected sequence, we observe that all the three regularization approaches give very similar reconstructed excitation fields, which are in very good agreement with the target excitation field [see Fig. 4]. This surprising result can be partly explained from the analysis of Fig. 3 showing that the reconstruction points are rather distant from each other. This probably makes the reconstruction easier over this relatively long sequence compared to the impact duration.

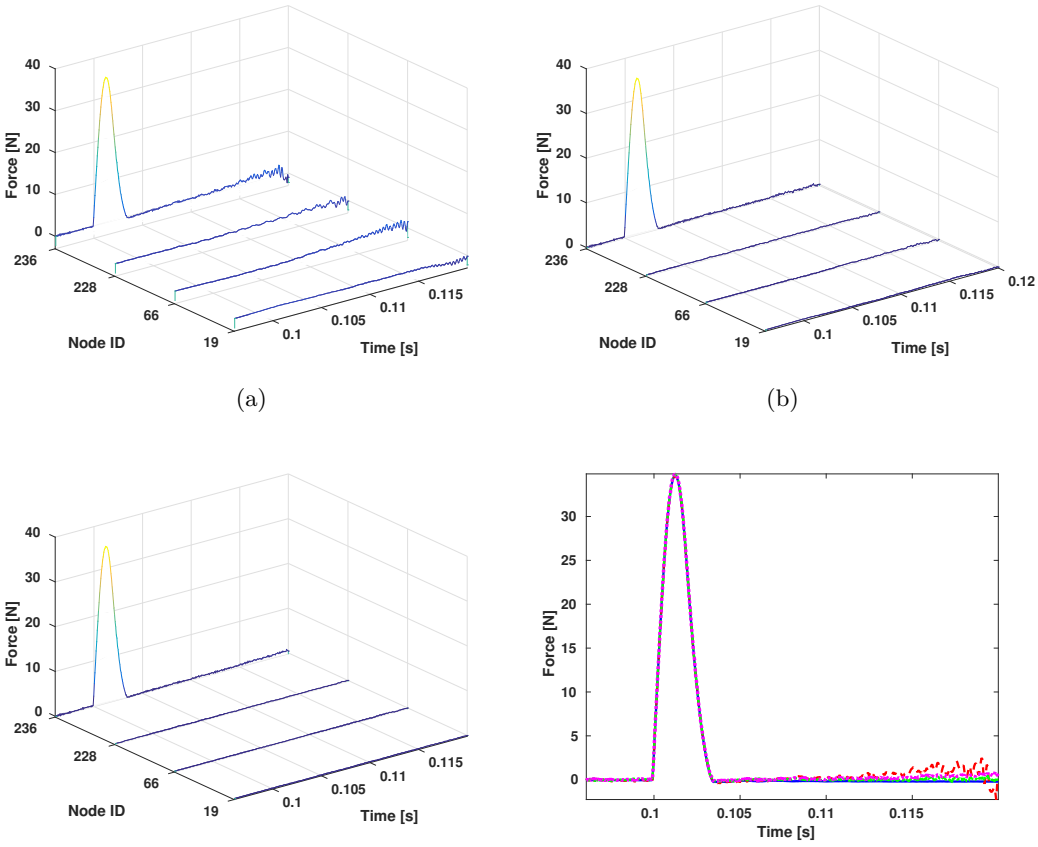

Figure 4: Reconstruction of the excitation field corresponding to a hammer impact over 24 ms – (a) Waterfall representation - mTIK regularization, (b) Waterfall representation - mLASSO regularization, (c) Waterfall representation - ST regularization for $(p, q) = (2, 0.5)$ and (d) Identified time signal at excitation point – (—) Reference signal and (– –) Tikhonov regularization, (– · –) LASSO regularization and (· · ·) ST regularization

Over a shorter duration, however, the results significantly differ. Indeed, when the reconstructions are performed on a sequence of 5.4 ms, obtained reconstructions show that, in this particular situation, only ST regularization allows obtaining a consistent space-time reconstruction of the target excitation field [see Fig. 5].

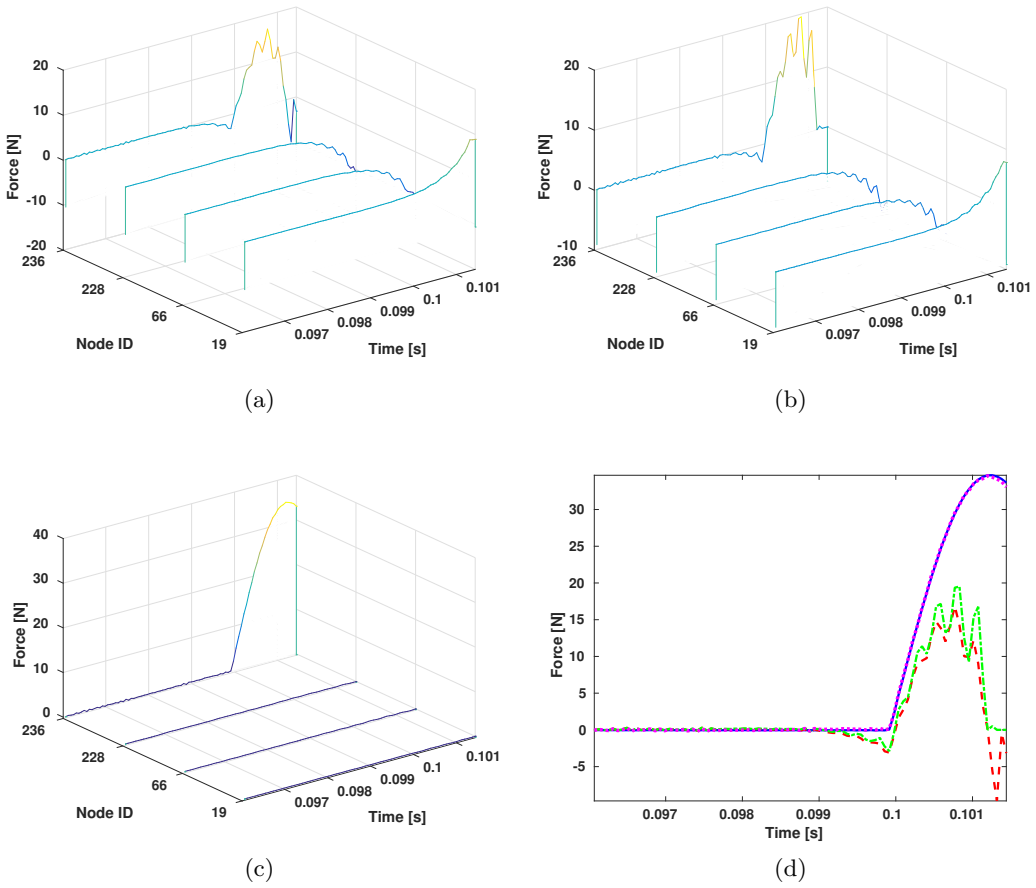

Figure 5: Reconstruction of the excitation field corresponding to a hammer impact over 5.4 ms – (a) Waterfall representation - Tikhonov regularization, (b) Waterfall representation - LASSO regularization, (c) Waterfall representation - ST regularization for $(p, q) = (2, 0.5)$ and (d) Identified time signal at excitation point – (—) Reference signal and (– –) Tikhonov regularization, (– · –) LASSO regularization and (· · ·) ST regularization

Consequently, this experimental application clearly indicates that properly exploiting simultaneously the space-time characteristics of excitation sources is beneficial in terms of quality and robustness of reconstructed solutions.

4. Conclusion

The practical interest of taking advantage of one's prior knowledge of the space-time characteristics of the sources to identify has been demonstrated in this contribution through a real-world application. More specifically, it has been clearly established that developing a regularization strategy based on the definition of a space-time regularization term allows improving the quality and robustness of reconstructed excitation sources.

References

[1] Lourens E, Reynders E, De Roeck G, Degrande G and Lombaert G 2012 *Mech. Syst. Signal Pr.* **27** 446
[2] Sturm M, Moorhouse A T, Alber T and Li F F 2012 *Proc. ISMA 2012*
[3] Jacquelin E, Bennani A and Hamelin P 2003 *J. Sound Vib.* **265**(1) 81
[4] Mao Y M, Guo X L, and Zhao Y 2010 *Exp. Mech.* **34**(3) 82

[5] Boyd S and Vandenberghe 2004 *Convex optimization* (Cambridge: Cambridge University Press)
[6] Ginsberg D and Fritzen C P 2014 *Proc. ISMA 2014*
[7] Qiao B, Zhang X, Gao J, Liu R and Chen X 2017 *Mech. Syst. Signal Pr.* **83** 509
[8] Grasmair M 2010 *J. Math. Anal. Appl.* **365**(1) 19
[9] Qiao B, Zhang X, Gao J, Chen X 2016 *J. Sound Vib.* **376** 72
[10] Turco E 2005 *Int. J. Numer. Meth. Eng.*
[11] Aucejo M, De Smet O and Deü J-F 2019 *Mech. Syst. Signal Pr.* **118** 549
[12] Aucejo M and De Smet O 2016 *Mech. Syst. Signal Pr.* **66-67** 120
[13] Gramfort A, Kowalski M and Hämäläinen M 2012 *Phys. Med. Biol* 57 1937
[14] Aucejo M and De Smet O 2017 *Mech. Syst. Signal Pr.* **85** 730
[15] Chung J and Hulbert G M 1993 *J. Appl. Math.* **60** 371
[16] Erlicher S, Bonaventura L and Bursi O 2002 *Comput. Mech.* **28** 83